antibonding between C and O atoms and bonding between Li and C. In addition there is some σ-bonding from the C atom lone pair toward the Li^+ ion.

In this description, the electron donor molecule is CO^-, both for the π bond and for the σ bond, while Li^+ is the electron acceptor. The Li^+CO^- complex we are describing is a pure example of an "intimate ion pair" isolated as a complex. In this description we see from the Mulliken charges described in part 3 for LiCO that 0.507 e (1 − 0.493) is transferred from CO^- to Li^+ in the π^* orbital and 0.298 e is transferred in the same direction in the σ bond. Hence the Li^+ charge is almost completely neutralized by the charge transfer but the valence electron transferred back to Li^+ has considerably more p character than s character, as it would have in an ordinary (Li, CO) no bond state (for example, in the $^2\Sigma$ electronic state of Li–CO).

According to this model, the electron transferred into the antibonding π_{CO}^* orbital in CO^- will reduce the force constant from that in CO because occupation of this extra antibonding orbital reduces the bond order from 3 in CO to 2.5 in CO^-. Hence the force constant ratio is predicted to be $K_R/k_r = 2.5/3 = 0.83$. In the charge transfer structure ψ_1, this electron is in the extended π^* antibonding orbital given above. It is still antibonding between C and O, to the same extent, so the predicted force constant ratio is still 0.83. This prediction compares very favorably with the value in Table I for the 6-31G* calculation (0.82) *and* from experiment ($K_R/k_r = 0.84$).

If the electron transferred from Li goes into the π^* orbital, and if the 2p AOs from all three atoms appear in π^* with equal coefficients as indicated above, then we might expect the p electron density on Li^+ to be 0.33 instead of 0.50, as shown above. To us, this difference does not appear to be unreasonable.

Perhaps the clearest indication of the charge transfer character of the $^2\Pi$ ground state for Li^+CO^- comes from the discussion in section III of the dependence of the calculated ratio, ω/ω_0, for the CO stretching frequencies on the Li–C distance. The $Li^+\cdots CO^-$ separated ion pair will have an energy $I_{Li} - E_{CO}$ (I is the ionization potential of Li; E is the electron affinity of CO) above the energy of separated ground state atoms, Li + CO [or about 5.39 − 0 ≃ 5.4 eV above Li(^{2}S) + CO]. The coulomb attraction, C, and valence interaction, V, stabilize the ion pair ($C \simeq 5.0$ eV at $R_{LiC} \sim 2.0$ Å; $V \simeq 0.5$ eV), so that the $^2\Pi$ Li^+CO^- curve has an avoided crossing with the purely dissociative $^2\Pi$ Li(^{2}P) + CO($^1\Sigma$) curve (see Figure 13.1 of reference 23 for a discussion of this situation in the analogous Li^+F^- charge transfer complex). According to the results quoted above for ω/ω_0, this avoided crossing occurs for R_{LiC} between 2.1 and 2.5 Å, according to our calculation here. This interaction between the ion pair Li^+CO^- $^2\Pi$ state and the dissociative $^2\Pi$ Li(^{2}P) + CO($^2\Sigma$) state appears to be the simplest explanation both for the stability of the $^2\Pi$ state and for its "avoided crossing" character.

Once we realize the ion pair nature of the Li^+CO^- interaction, it is easy to understand the other complexes formed and their infrared spectra. In the 1:2 $Li(CO)_2$ complex, for example, the Li atom donates its electron to two CO molecules which share it equally in π_{CO}^* orbitals. The extended π^* orbital involves both π_{CO}^* orbitals and the Li 2p orbitals and is antibonding between both pairs of C and O oribtals and bonding between Li and C atoms. The antibonding contribution of the electron to the CO bond is expected to be about one-half of that in Li^+CO^-, so the force constant ratio K_R/k_r is predicted to be 2.75/3.0 = 0.92 for $Li(CO)_2$, compared with 0.85 from the 6-31G* calculation or 0.74 from experiment. In fact, the latter values suggest that the antibonding contribution from the electron in the extended π^* orbital is the same as in the corresponding orbital for Li^+CO^-, which is probably more reasonable than to picture the CO molecules in competition for this electron.

Finally, we note that in the 2:1 Li_2CO complex, two electrons are donated to the antibonding π_{CO}^* orbital of CO^-, or to the corresponding extended π^* orbital in $Li^+\text{--}CO^{2-}\text{--}Li^+$. Hence, the bond order is only 2, and the value of K_R/k_r is predicted to be 2/3 = 0.67. The two electrons are contained in the extended π^* orbital, which can hold a total of 4 electrons because of the x and y degeneracy, so the electronic states are like those for O_2, with the $^3\Sigma^-$ state expected to be lowest in energy. The predicted ratio of force constants agrees reasonably well with the value ($K_R/k_r \simeq (\omega/\omega_0)^{1/2} \simeq 0.77$) for the 6-31G* calculation.

Acknowledgment. Willis B. Person would like to acknowledge the hospitality and support provided him during the course of this work. We are grateful to J. P. Perchard for many stimulating discussions. The calculations have been performed at CIRCE (CNRS).

Registry No. LiCO, 103173-65-5; $Li(CO)_2$, 105121-67-3; Li_2CO, 105139-44-4.

Molecular Dynamics Simulations of α-D-Glucose

J. W. Brady

Contribution from the Department of Food Science, Cornell University, Ithaca, New York 14853.
Received January 16, 1986

Abstract: Molecular dynamics simulations were performed for α-D-glucose in vacuo in the $^1C_4$ and $^4C_1$ conformations, using the most developed semiempirical potential energy surface available for carbohydrates, as a test of the suitability of this function for representing molecular motions and to explore the dynamical fluctuations of pyranoid rings. Contrary to the assumption of rigid-ring geometry frequently employed in conformational studies of polysaccharides, the glucopyranose molecules were found to exhibit considerable flexibility and to undergo a variety of conformational fluctuations and even transitions. As in previous energy minimization studies, the $^4C_1$ conformer was found to be more stable, and the free-energy difference between the two forms was calculated to be 2.44 kcal/mol, in accord with previous estimates. The mean dynamical structure for the glucose molecule with this potential energy is acceptably close to the experimentally determined crystal structure, with the most important deviation being in the ring geometry about the C5 carbon atom and the O5 oxygen atom.

I. Introduction

In recent years the structure and dynamics of polypeptides, proteins, and nucleic acids have received considerable attention, both experimentally and theoretically.[1,2] The most abundant of biological molecules, however, the carbohydrates, have not been the focus of intensive theoretical study. A number of conformational energy studies of simple sugars and disaccharides have elucidated the main features of oligosaccharide conformational

(1) Karplus, M.; McCammon, J. A. *Annu. Rev. Biochem.* **1983**, *53*, 263.

(2) Scheraga, H. A. *Biopolymers* **1981**, *20*, 1877.

0002-7863/86/1508-8153$01.50/0

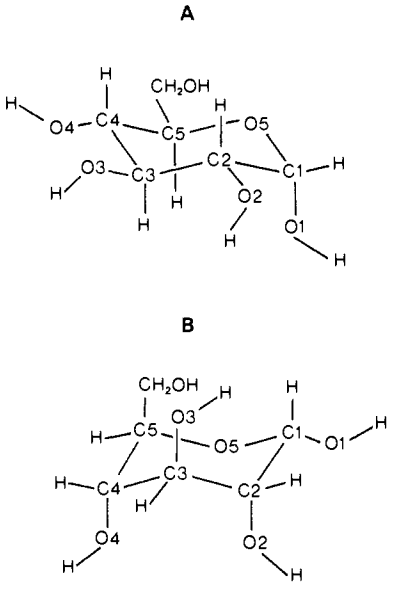

Figure 1. α-D-Glucose: (A) in the $^4C_1$ conformation, (B) in the $^1C_4$ conformation.

preferences,[3] but the dynamics and solvation of these molecules are still relatively unexplored.[4] Currently there is interest in the role of oligosaccharides in glycoproteins, aggregation, adhesion, and antigenicity, and molecular dynamics simulations of the aqueous solvation of various simple sugars and disaccharides could contribute to a fundamental understanding of such processes. As a preparation for such simulations, molecular dynamics calculations are reported here of the vacuum motions of α-D-glucopyranose in the $^4C_1$ and $^1C_4$ conformations using the most extensively tested of the potential energy surfaces reported in the literature.

II. Procedures

In the simulations reported here, Newton's equations of motion were solved numerically for the $^4C_1$ and $^1C_4$ conformations of the simple sugar α-D-glucose in the pyranose ring form, shown in Figure 1. While several potential surfaces for pyranose sugars have been proposed for use in conformational energy studies,[5-7] the one developed by Rasmussen and co-workers[8-11] is to date the most extensively tested and perhaps the most suited for molecular dynamics simulations. The particular potential surface used in the present studies is designated PEF 422 by these authors[8] and has the form

$$V = \frac{1}{2}k_b(b - b_0)^2 + \frac{1}{2}k_\theta(\theta - \theta_0)^2 + \tfrac{1}{2}k_\phi[1 + \cos(n\phi)] + \sum_{i>j}\left[\epsilon_{ij}\left(\frac{r_{ij}^0}{r_{ij}}\right)^{12} - 2\,\epsilon_{ij}\left(\frac{r_{ij}^0}{r_{ij}}\right)^{6} + \frac{q_i q_j}{\epsilon_D r_{ij}}\right] \quad (1)$$

incorporating harmonic bond stretching and bending terms with force constants k_b and k_θ, a torsional term with periodicity n and force constant k_ϕ, Lennard-Jones-type nonbonded interactions, and a Coulomb term between partial charges q_i and q_j with a dielectric constant ϵ_D of 3.0. No explicit hydrogen bond term is included in this force field. In the present study, bond lengths were kept fixed using a constraint technique (see below), but this term is included in eq 1 for completeness. Nonbonded and Coulomb interactions were computed between all atoms not bonded to one another or to a common atom. The magnitude of the atomic charges used in the Coulomb interaction were chosen from ab initio calculations.[9] The exact value of the charges used were found to have only a small effect upon the minimum energy conformation for glucopyranose,[8] which has also been found to be true for alanine dipeptide;[12] however, for solution simulations, it will be necessary to represent these partial charges as accurately and consistently as possible. While earlier versions of the potential energy function developed by these workers contained a nonnegligible explicit torsional energy,[13] in their final potential surface the torsional force constants have been made effectively zero and Lennard-Jones interactions alone account for hindered rotations.[14] Note that the definition of sign used here for dihedral angles is opposite to that employed in ref 13 (p 8). All of the molecule's hydrogen atoms were included explicitly in the simulations; that is, "united" or "extended" atom representations[15] were not used. The final set of partial atomic charges, Lennard-Jones parameters, force constants, and equilibrium bond lengths and angles developed by these workers are summarized in Table I.

Table I. Potential Energy Parameters

a. Bond Stretches

bond type	k_b (kcal/mol·Å^2)	b_0, (Å)
O-C	719.868	1.410
C-C	510.026	1.509
O-H	1070.003	0.955
C-H	669.917	1.093

b. Bond Angles

angle type	k_θ (kcal/rad^2)	θ_0 (deg)
O-C-O	59.989	109.47
O-C-C	99.902	109.47
O-C-H	99.902	109.47
C-O-C	70.027	103.13
C-O-H	80.065	103.13
C-C-C	49.951	109.47
C-C-H	70.983	109.47
H-C-H	75.046	109.47

c. Dihedral Angles

angle type	k_ϕ (kcal/mol)
X-O-C-Y	0.000956
X-C-C-Y	0.000956

d. van der Waals Interactions

interaction type	ϵ_{ij} (kcal/mol)	r_{ij} (Å)
O-O	0.300	3.00
O-C	0.300	3.05
C-C	0.100	3.50
O-H	0.100	2.95
C-H	0.100	3.15
H-H	0.300	2.75

e. Partial Charges

atom type	charge
oxygen (both ring and hydroxyl)	−0.465
anomeric carbon C1	0.235
all other carbons	−0.015
hydroxyl hydrogens	0.337
all other hydrogens	0.135

In the present study the equations of motion for the Cartesian coordinates for the atoms of the glucose molecule were integrated numerically using the general molecular mechanics code CHARMM, developed by Karplus and co-workers.[15] A Verlet integration scheme[16] was used with a step size of 0.5×10^{-15} s. In these calculations, the bond lengths were kept fixed at their crystallographic values using the constraint procedure SHAKE,[17] with an error tolerance of 10^{-6}. Trajectories were initiated by assigning velocity components randomly selected from a thermal distribution to the sugar atoms, whose initial coordinates were taken to be

(3) Rees, D. A.; Morris, E. R.; Thom, D.; Madden, J. K. In *The Polysaccharides*; Aspinall, G. O., Ed.; Academic Press: New York, 1982; Vol. 1.
(4) Suggett, A. In *Water: A Comprehensive Treatise*, Franks, F., Ed.; Plenum Press: New York, 1975; Vol. 4.
(5) Rao, V. S. R.; Vijayalakshmi, K. S.; Sundararajan, P. R. *Carbohyd. Res.* **1971**, *17*, 341.
(6) Rees, D. A.; Smith, P. J. C. *J. Chem. Soc., Perkin Trans. 2* **1975**, 830.
(7) Goebel, C. V.; Dimpfl, W. L.; Brant, D. A. *Macromolecules* **1970**, *3*, 644.
(8) Rasmussen, K. *Acta Chem. Scand., Ser. A* **1982**, *36*, 323.
(9) Melberg, S.; Rasmussen, K.; Scordamaglia, R.; Tosi, C. *Carbohyd. Res.* **1979**, *76*, 23.
(10) Melberg, S.; Rasmussen, K. *Carbohyd. Res.* **1980**, *78*, 215.
(11) Melberg, S.; Rasmussen, K. *J. Mol. Struct.* **1979**, *57*, 215.
(12) Pettitt, B. M.; Karplus, M. *J. Am. Chem. Soc.* **1985**, *107*, 1166.
(13) Kildeby, K.; Melberg, S.; Rasmussen, K. *Acta Chem. Scand., Ser. A* **1977**, *31*, 1.
(14) Niketić, S. R.; Rasmussen, K. *The Consistent Force Field: A Documentation* (Lecture Notes in Chemistry); Springer-Verlag: Heidelberg, 1977; Vol. 3.
(15) Brooks, B. R.; Bruccoleri, R. E.; Olafson, B. D.; States, D. J.; Swaminathan, S.; Karplus, M. *J. Comput. Chem.* **1983**, *4*, 187.
(16) Verlet, L. *Phys. Rev.* **1967**, *159*, 98.
(17) van Gunsteren, W. F.; Berendsen, H. J. C. *Mol. Phys.* **1977**, *34*, 1311.

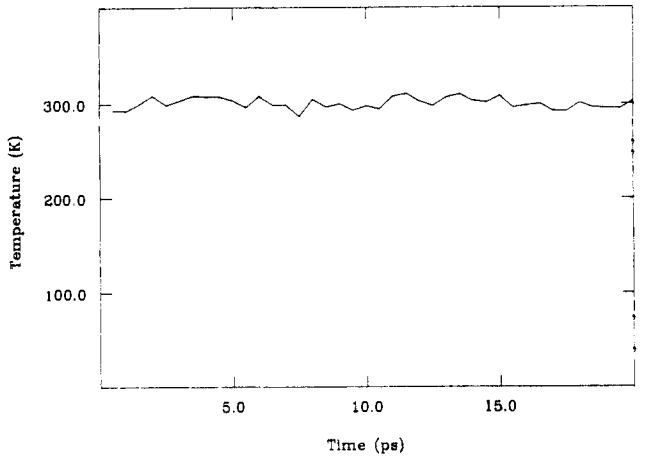

Figure 2. History of the molecular temperature for a representative trajectory. Each point represents the average temperature for the previous 0.5 ps of dynamics.

those determined crystallographically in the case of the $^4C_1$ conformation,[18] and in the case of the $^1C_4$ conformer were those for an idealized geometry. For each conformation, an ensemble of 12 trajectories of 20-ps duration were computed, giving 240 ps of dynamics. Each trajectory was equilibrated for 40 ps, with periodic temperature scalings during the equilibration period to bring the system to a temperature acceptably close to the desired temperature of 300 K. During the subsequent 20 ps of data collection, no scalings were made, and the energy of the system was conserved to better than one part in 10^5. Phase space points were saved at every fifth time step for subsequent analysis. Ensembles of 12 trajectories would appear to be adequate for the properties under examination for this system, since both structural and energetic properties for individual simulations fluctuated by only small amounts from the ensemble averages.

III. Results and Discussion

The slow exchange of energy between internal modes, as well as the exchange between kinetic and potential energy, gives rise to moderately large temperature fluctuations in a small isolated system such as glucose. The magnitude of these fluctuations depends upon the time over which the "temperature" is averaged, and will approach zero as the time-averaged temperature approaches the true thermodynamic temperature for that trajectory. Figure 2 shows the time history of the short-term temperature for a typical $^4C_1$ trajectory which had an average temperature of 300.3 K. In this figure, each point plotted is the average temperature for the previous 0.5 ps of the trajectory. As expected, the temperature fluctuates, in the present example between a high of 311.0 K and a low of 286.7 K. These long-lived fluctuations in system temperature, along with the time scale for equipartition of system energy, complicate attempts to scale trajectory temperatures precisely to 300 K, and in practice it was necessary to accept a small spread in trajectory temperatures about the desired 300 K. For the studies reported here, no trajectories were used whose temperature, averaged over the entire run, differed from 300 K by more than 3.5 K. The ensemble average temperature was 299.9 K for both conformations studied.

The time-averaged structure of the $^4C_1$ conformer is compared in Table II to the structure determined by neutron diffraction[18] using selected internal coordinates. The averaging over trajectories used to compile Table II has not obscured any structural features of the molecule; the time and ensemble averaged structure is also a "real" structure rather than the result of combining together two or more different structures, as was determined by examining structures for individual trajectories for short periods, and for different orientations of the exocyclic group (see below). As can be seen, the dynamical structure is quite close to that for the crystal. The dynamical averages for the bond angles are in most cases larger than the crystal values, and also the minimum energy values selected for the energy function (Table I). It might also

Table II. Mean Structure of α-D-Glucose in the $^4C_1$ Conformation as Computed from Molecular Dynamics Simulations

angle	mean value from dynamics	RMS fluctuation	exptl value[a]
C1-C2-C3-C4	-51.6	7.89	-51.3
C2-C3-C4-C5	49.7	8.13	53.3
C3-C4-C5-C6	-171.1	9.85	-176.6
C3-C4-C5-O5	-50.3	10.15	-57.5
C4-C5-O5-C1	56.3	10.58	62.2
C5-O5-C1-C2	-58.7	9.36	-60.9
O5-C1-C2-C3	54.6	8.88	54.1
C1-C2-C3-O3	-174.0	8.97	-172.0
C2-C3-C4-O4	172.9	9.05	175.3
O1-C1-C2-O2	56.7	10.85	56.9
O1-C1-C2-C3	-68.4	10.00	-68.7
C1-C2-C3	110.4	4.32	111.1
C2-C3-C4	110.9	4.15	109.8
C3-C4-C5	111.9	4.33	111.1
C4-C5-C6	114.0	4.62	111.5
C4-C5-O5	110.5	4.54	108.7
C5-O5-C1	115.4	4.35	113.7
O5-C1-O1	110.7	5.83	111.5
C1-C2-O2	111.3	4.76	110.9
C2-C3-O3	110.6	4.83	108.1
C3-C4-O4	111.2	4.77	108.2
C5-C6-O6	112.7	4.75	109.9

[a] Values calculated from ref 29.

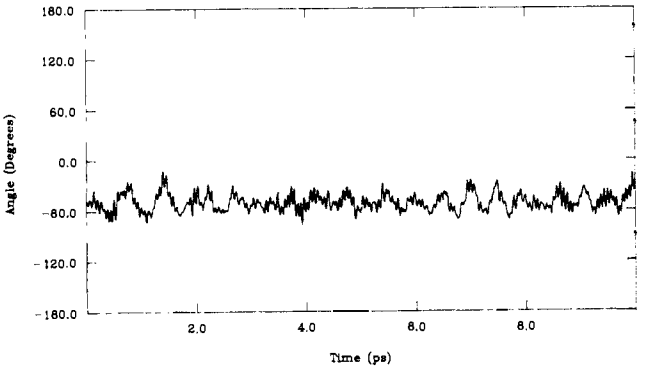

Figure 3. History of the dihedral angle C3-C4-C5-O5 for a representative $^4C_1$ trajectory.

be noted that there is a small shift in the dynamically averaged structure away from the minimum energy structure for the same potential;[11] the angle O5-C1-O1, for example, shifted from 111.6 to 110.7°, and C5-O5-C1 from 113.5 to 115.4°. Unfortunately, the significance of such shifts are unclear because of the fixed bond length in the dynamical simulation. For the dihedral angles, the most substantial differences occur for the angles C3-C4-C5-C6, C3-C4-C5-O5, and C4-C5-O5-C1. These three angles define the geometry in the region around the C6 "side chain" (i.e., the CH_2OH group on C5) and the ring oxygen, and the directions of the deviations indicate a slight deformation of the ring about the C5-O5 bond, toward a "flatter" geometry than observed experimentally. Most pyranose ring forms of monosaccharides in the crystalline state, including α-D-glucose, exhibit a sharpening of the ring at the O5 ring oxygen to values closer to the ideal value of 60° than the flatter values in the 52-57° range characteristic of the C-C-C-C and C-C-C-O dihedral angles[19] (see Table II). This feature of the ring structure is not preserved in the dynamical simulations using the PEF 422 potential function. It should also be noted that the largest deviation in bond angles occurs here as well, in the C4-C5-C6 angle. The origin of these deviations is unclear (they could, for example, be due to the absence of crystal neighbors), but if spurious may well have been facilitated by the effective lack of explicit rotational barriers in the torsional energy term.

(18) Brown, G. M.; Levy, H. A. *Science* **1965**, *147*, 1038.

(19) Jeffrey, G. A. In *Carbohydrates in Solution* (Advances in Chemistry Series, No. 117); American Chemical Society: Washington, D.C., 1973.

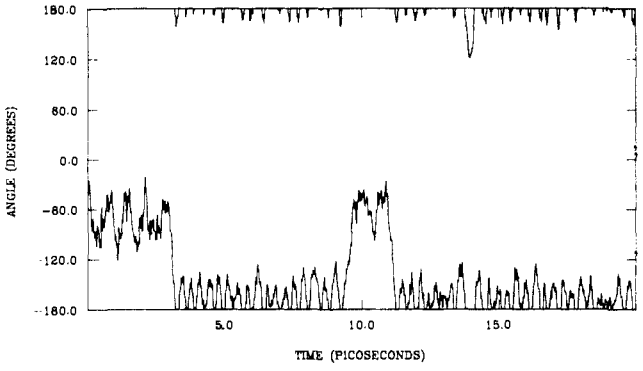

Figure 4. History of the dihedral angle C4–C5–C6–O6 describing the orientation of the exocyclic group for a representative $^4C_1$ trajectory.

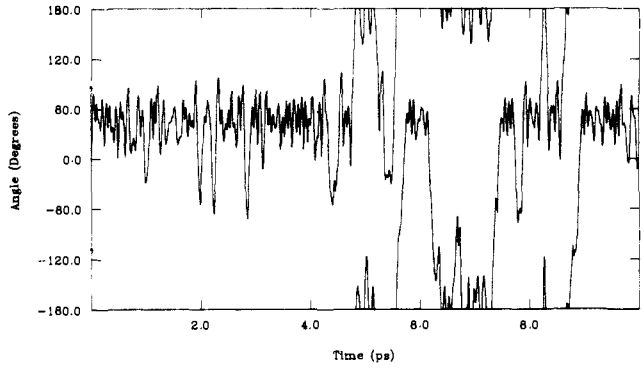

Figure 5. History of the dihedral angle O5–C1–O1–H describing the orientation of the hydroxyl group on the anomeric carbon for a representative $^4C_1$ trajectory.

The pyranose rings in these simulations, rather than being nearly rigid as has often been assumed in the past, were found to exhibit considerable flexibility, undergoing a variety of fluctuations at 300 K with this potential energy function. Figures 3–5 display time histories for the first 10 ps of several of the molecular dihedral angles for a typical trajectory. As can be seen from these figures, these angles undergo oscillations at several characteristic frequencies, with the fluctuations in those angles involving the ring oxygen being greater than those for the other side of the ring (e.g., C2–C3–C4–C5). Such molecular flexibility is consistent with the oservation of French and Murphy that a variety of ring conformations occur in the known crystal structures of oligosaccharides, implying considerable flexibility resulting in environmentally induced low-energy geometric distortions.[20]

The greatest fluctuations occur in the torsional angle C4–C5–C6–O6, which is shown in Figure 4 for the entire 20 ps of the trajectory. Unlike the ring dihedrals, this side-chain dihedral angle has three low-energy values accessible to it, corresponding to three positions of the O6 oxygen, two gauche (±60°) and one anti (180°) relative to the C4 atom, and the barrier to rotation is sufficiently low as to allow frequent transitions at 300 K. In Figure 4, three such transitions can be seen. It should be noted that all three allowed values, −60, 60, and 180°, are for the $^4C_1$ conformer; rotations of this exocyclic group do not affect the ring conformation. When in the well near 180°, the ensemble average value for this dihedral angle was −168.3°, indicating a slight rotation of the exocyclic group oxygen O6 away from the ring oxygen O5. The crystal value for this dihedral angle is −170.3°, very close to the trajectory average, with the exocyclic hydroxyl group engaged in an intermolecular hydrogen bond.[18] When the dihedral angle was in the well near −60°, its ensemble average value was −68.4°. When averaged over the entire ensemble of 12 runs, it was found that these three values for this dihedral angle do not occur with equal probability. For the $^4C_1$ trajectories, this dihedral angle was in the well near −60° approximately 38% of the time, in the well near 180° about 55% of the time, and only spent approximately 7% of the time in the well at +60°. During the 12 runs of 20 ps, 50 transitions in this dihedral occurred, which is 0.21 transition/ps or 1 transition approximately every 4.8 ps.

The molecular conformation with the C4–C5–C6–O6 dihedral angle at −60° can in principle allow an internal hydrogen bond to form between the O6 hydrogen and the oxygen of the O4 hydroxyl group, and thus might be expected to have a lower energy in vacuo than the anti conformer, where such an internal hydrogen bond is not possible (Marchessault and Perez have shown that this arrangement is not significantly destabilized by oxygen–oxygen van der Waals repulsions[21]). It has been suggested, however, that such a hydrogen bonding tendency might be opposed by an unfavorable close parallel alignment of the C4–O4 and C6–O6 hydroxyl groups, referred to as "peri interactions" or "syn-axial interactions" (similar to the Hassel–Ottar effect)[21]. The expectation of internal hydrogen bonding in vacuo is supported by the experimental findings of Lemieux and Brewer[22] that in 1,2-dichloroethane solution a hexapyranose analogue of α-D-glucose maintained a conformational equilibrium between the three allowed conformers approximately in the proportions

$$0.5\ (-60°) \rightleftarrows 0.35\ (180°) \rightleftarrows 0.15\ (+60°) \qquad (2)$$

with the internally hydrogen-bonded form favored. While a conformational equilibrium such as eq 2 was found for the trajectories reported here, the relative order of the dominant forms was reversed. Furthermore, the distribution is quite different from that found in a survey of known crystal types, where the "gauche–trans" conformer (+180°) and "gauche–gauche" (+60°) conformer were found in the ratio 40:60, and where the conformer at −60° does not occur. In the simulations, the conformer at −60° was found to have a higher potential energy, averaged over all time spent in this well, than the anti conformer by about 0.25 ± 0.19 kcal/mol. The anti conformer was found to have a lower entropy, however (see below), negating some of the energy advantage; the free-energy difference between the two orientations of the exocyclic group, calculated from the trajectories, was found to favor the anti conformer by 0.12 kcal/mol (note, however, that the magnitude of this number is less than the error in the energy estimate, leaving the sign in question). Experiment[22] and intuition would indicate a shift further in favor of the anti conformer in aqueous solution; it will be interesting to see if solution calculations with this potential are consistent with this expectation.

The hydroxyl groups on the ring carbon atoms underwent frequent transitions between their allowed conformations, sometimes rotating through a full 360° or more before again becoming briefly trapped in one of the wells. An example of the time history of one of these angles for a representative trajectory is presented in Figure 5, showing several conformational transitions. No attempt was made to quantitate the frequency of these transitions, owing in part to the difficulty of defining a "transition" for a rapidly rotating group which may pass directly through a conformational well without reversing its direction. These transitions occur often for all of the molecule's hydroxyl groups, however, and there is virtually no period of the trajectories during which one or more are not in the process of rearranging. As might be expected, transitions in these dihedral angles often exhibit strong short-term correlations, since some orientations of one group might inhibit the free rotation of an adjacent group until it moved or was knocked out of the way. Hydroxyl rotations would clearly be affected by the presence of solvent, since reorientation would involve an exchange of hydrogen bond partners, but solution simulations, which are to be undertaken soon, will be required to determine the importance of solvent for these transitions.

Trajectories were also computed for molecules in the $^1C_4$ conformation at the same temperature. Obtaining an ensemble of 12 trajectories for this conformer was difficult, since fewer than one trajectory in four survived in this conformation through both the equilibration period and 20 ps of subsequent dynamics. Most

(20) French, A. D.; Murphy, V. G., *Polymer* **1977**, *18*, 489.

(21) Marchessault, R. H.; Perez, S. *Biopolymers* **1979**, *18*, 2369.
(22) Lemieux, R. V.; Brewer, J. T. In ref 19.

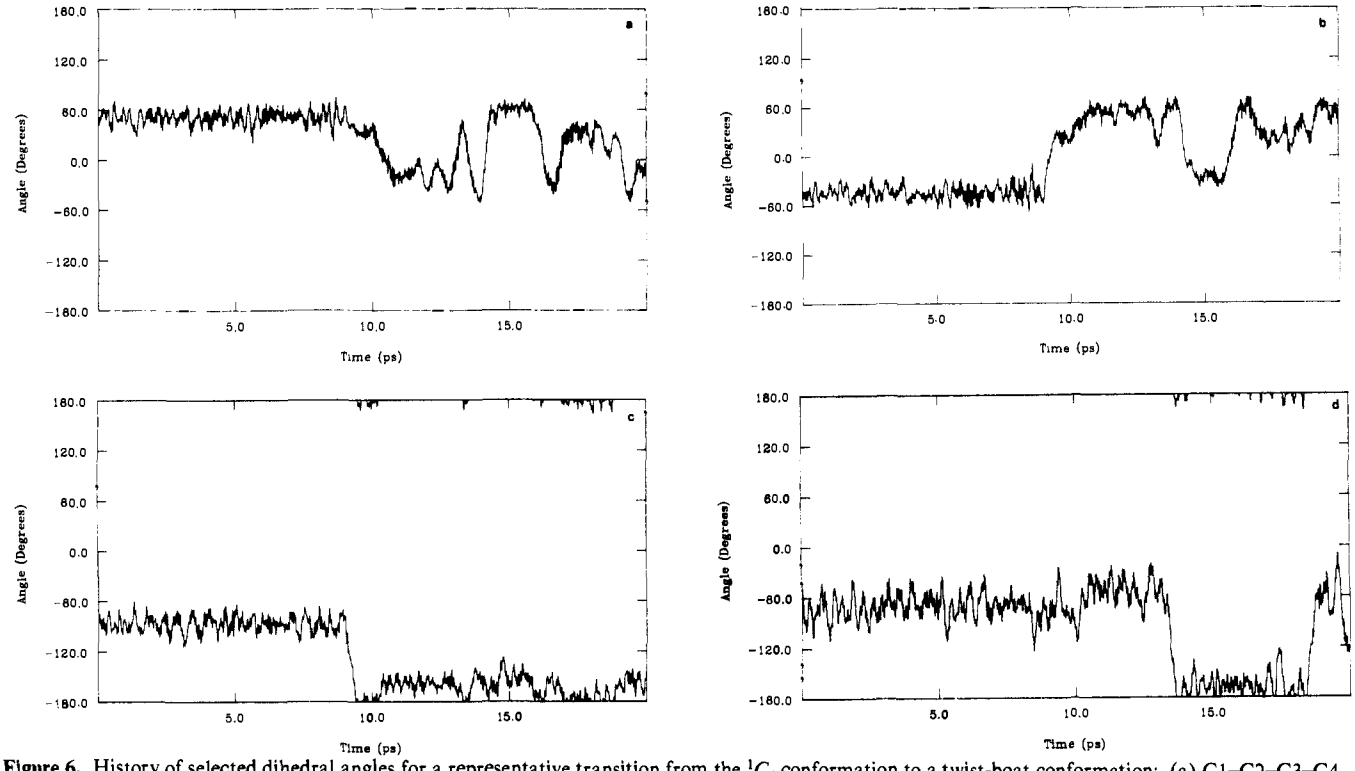

Figure 6. History of selected dihedral angles for a representative transition from the $^1C_4$ conformation to a twist-boat conformation: (a) C1–C2–C3–C4, (b) C2–C3–C4–C5, (c) C3–C4–C5–C6, (d) C4–C5–C6–O6.

trajectories underwent spontaneous transitions to the more favorable twist-boat, half-chair, and $^4C_1$ conformers. An example of such a transition is shown in Figure 6, which displays the changes in the dihedral angles C1–C2–C3–C4, C2–C3–C4–C5, and C3–C4–C5–C6, and Figure 7, which illustrates the history of the Cremer–Pople pucker parameters.[23] While the histories of the dihedral angles exhibit a number of transitions, these involve primarily oscillations between various near-boat and twist-boat forms; the basic transition from chair to boat is direct and the molecule does not return to the $^1C_4$ arrangement (Figure 7). As seen from the time history of the dihedral angle C4–C5–C6–O6 (Figure 6d), side-chain reorientation was not initially involved in the transition, but this group subsequently underwent transitions after distorting away from the $^1C_4$ conformation.

These transitions in ring conformation occur as a result of the fact that the $^4C_1$ conformer has a lower potential energy than the $^1C_4$ and a greater configurational entropy. Both of these effects are primarily the result of increased steric crowding in the undistorted $^1C_4$ conformation, in which the C6 sidechain and three of the four ring hydroxyl groups are in axial positions, giving rise to possibly unfavorable nonbonded interactions between these bulky axial groups (see Figure 1). The difference in the mean potential energies for the two ensembles was 2.11 ± 0.28 kcal/mol, almost entirely due to a higher angle energy for the $^1C_4$ conformer, resulting from bond angle strains as the molecule deforms to avoid these steric overlaps. The mean van der Waals energies for the two conformers, averaged over the ensembles of simulations, are essentially identical, within statistical error, since the molecule distorts to avoid strongly repulsive overlaps and in the process relieves some of the nonbonded repulsion. There is a further gain in nonbonded energy due to the formation of a very stable hydrogen bond between the hydroxyl hydrogen on O2 and the O4 oxygen atom once the ring has distorted. Such a hydrogen bond is not possible in the $^4C_1$ conformation. Several of the dihedral angles in the $^1C_4$ conformer (Table III) are significantly more distorted than in the $^4C_1$ conformation, but the energetic cost of this deformation is small because of the nearly zero force constants in the torsional energy term. The crowding of the axial groups and the formation of the intramolecular hydrogen bond also decrease the energetically allowed fluctuations, thus decreasing the configurational entropy of the conformation. The flexibility of the ring with this potential is such that the free energy difference eventually drives the molecule over to the more favorable conformer.

Table III. Mean Structure of α-D-Glucose in the $^1C_4$ Conformation as Computed from Molecular Dynamics Simulations

angle	mean value from dynamics	RMS fluctuation
C1–C2–C–C4	50.7	7.53
C2–C3–C4–C5	−44.7	8.27
C3–C4–C5–C6	−86.7	9.69
C3–C4–C5–O5	42.4	9.96
C4–C5–O5–C1	−50.2	9.96
C5–O5–C1–C2	58.1	9.17
O5–C1–C2–C3	−56.4	8.64
C1–C2–C3–O3	−71.1	9.22
C2–C3–C4–O4	81.1	9.80
O1–C1–C2–O2	−54.2	11.14
O1–C1–C2–C3	−177.6	9.48
C1–C2–C3	109.4	4.46
C2–C3–C4	111.9	4.37
C3–C4–C5	114.1	4.32
C4–C5–C6	116.5	4.54
C4–C5–O5	111.9	4.39
C5–O5–C1	116.4	4.38
O5–C1–O1	109.6	5.68
C1–C2–O2	113.1	4.71
C2–C3–O3	109.3	5.01
C3–C4–O4	110.2	4.76
C5–C6–O6	112.4	4.86

In general, the dynamical and fluctuational behavior of the internal coordinates for the $^1C_4$ conformation are similar to that seen for the $^4C_1$ conformer. An important exception to this observation is the dihedral angle C4–C5–C6–O6. For the $^1C_4$ conformation, the fluctuations in this coordinate were significantly smaller (see below) and the angle underwent fewer transitions. During the ensemble of 12 runs of 20-ps duration, only 10 transitions were observed, one-fifth the rate seen for the $^4C_1$ conformation. The molecule spent approximately 62% of its time in the well at −60°, which may allow some hydrogen bonding between

(23) Cremer, D.; Pople, J. A. *J. Am. Chem. Soc.* **1975**, *97*, 1354.

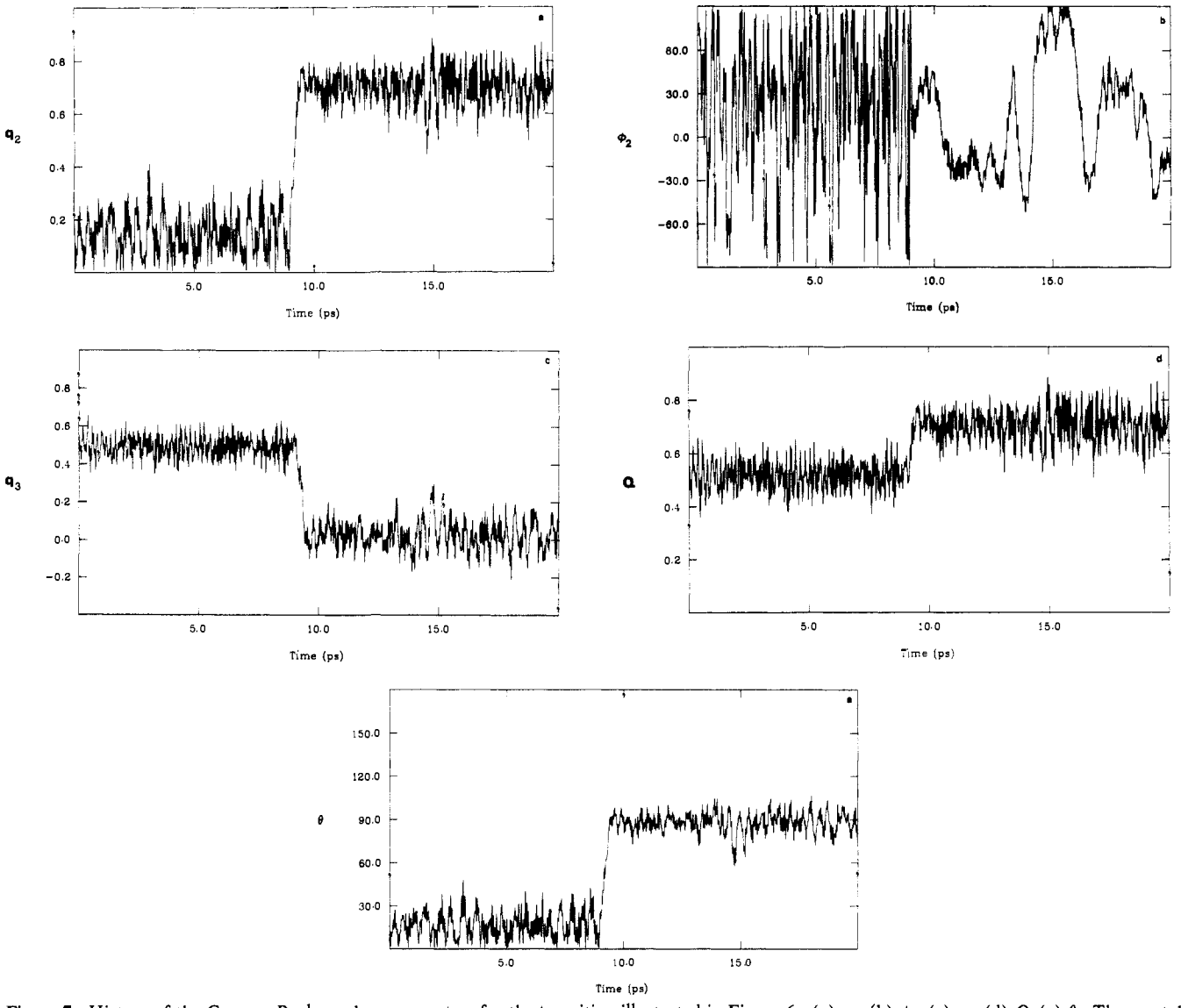

Figure 7. History of the Cremer–Pople pucker parameters for the transition illustrated in Figure 6: (a) q_2, (b) ϕ_2, (c) q_3, (d) Q, (e) θ. The crystal values for these parameters are as follows:[29] $q_2 = -0.0347$ Å; $q_3 = 0.5657$ Å; $Q = 0.5668$ Å; $\theta = 3.51°$; $\phi_2 = -36.9°$.

the O6 hydroxyl hydrogen and the O3 oxygen which cannot occur in the possibly sterically more favorable 180° conformation, where it spent only 38% of the trajectory time.

Using an approximate method developed by Karplus and Kushick,[24] it is possible to use molecular dynamics simulations such as these to estimate the entropy difference between two molecular conformations.[25] The method involves approximating the molecular potential energy as a quadratic function of a set of "important" molecular coordinates q. These coordinates are "important" in the sense that they describe the molecular conformation and are therefore possibly conformation dependent; coordinates presumed to be conformation independent, such as bond lengths in the present case, are not used. In this technique, the joint probability distribution function for the important coordinates is modeled as a multivariate Gaussian distribution, and the entropy difference between two configurations is calculated from the matrix of variances and covariances in the important coordinants, σ,

$$\sigma_{ij} = \langle (q_i - \langle q_i \rangle)(q_j - \langle q_j \rangle) \rangle \tag{3}$$

using the formula

$$\Delta S = \frac{k_B}{2} \ln \frac{\sigma(b)}{\sigma(a)} \tag{4}$$

where σ is the determinant of the matrix σ.

One problem with applying this technique to the present simulations is the frequent transitions in the dihedral angles describing the hydroxyl group orientations and the side-chain dihedral C4–C5–C6–O6. The large deviations in these angles from the minima of their potential wells and their passage over the intervening barriers clearly violate the harmonic expansion of the energy in terms of the internal coordinates, which is the basis for this procedure. It is thus not possible to use this approach to calculate the contribution of these rotating hydroxyl groups to the configurational entropy of the system. However, this method can be used to calculate the configurational entropy of the heavy atoms in the molecule, if each trajectory is broken up into separate segments corresponding to the periods during which the C4–C5–C6–O6 dihedral angle remained in one specific well. For example, the trajectory illustrated in Figure 4 was partitioned into four separate segments for the purpose of calculating the covariance in the fluctuations of this angle. In computing a mean fluctuation from the local average for the entire run, each segment was weighted in proportion to the fraction of the total run which it represented.

Glucose contains 12 heavy atoms; if all bond lengths are fixed at a known value, 18 internal coordinates are needed to specify the relative geometry of these 12 atoms. For the calculation of configurational entropies, a set of internal coordinates was selected consisting of 8 dihedral angles and 10 bond angles, which was

(24) Karplus, M.; Kushick, J. N. *Macromolecules* **1981**, *14*, 325.
(25) Brady, J.; Karplus, M. *J. Am. Chem. Soc.* **1985**, *107*, 6103.

Table IV. Set of "Important" Coordinates Used in Configurational Entropy Calculations

	Dihedral Angles	
1	$\phi(1)$	O1–C1–C2–O2
2	$\phi(2)$	O1–C1–C2–C3
3	$\phi(3)$	C1–C2–C3–O3
4	$\phi(4)$	C1–C2–C3–C4
5	$\phi(5)$	C2–C3–C4–O4
6	$\phi(6)$	C2–C3–C4–C5
7	$\phi(7)$	C3–C4–C5–C6
8	$\phi(8)$	C4–C5–C6–O6
	Bond Angles	
9	$\theta(1)$	O1–C1–C2
10	$\theta(2)$	C1–C2–O2
11	$\theta(3)$	C1–C2–C3
12	$\theta(4)$	C2–C3–O3
13	$\theta(5)$	C2–C3–C4
14	$\theta(6)$	C3–C4–O4
15	$\theta(7)$	C3–C4–C5
16	$\theta(8)$	C4–C5–C6
17	$\theta(9)$	C5–C6–O6
18	$\theta(10)$	C4–C5–O5

sufficient to completely specify the conformation of the molecule. The internal coordinates used here are listed in Table IV. It should be noted that this set is neither orthogonal or unique. From the calculated dynamics trajectories, the covariance matrices for these internal coordinates and their determinates were computed for both conformational ensembles. These covariance matrices averaged over the respective ensembles of 12 trajectories appear to be well converged, with averages over subsets giving results similar to the mean for the entire ensemble. This situation is quite different from that observed for vacuum conformations of the alanine dipeptide, where the considerable flexibility of the main-chain dihedrals required extensive averaging for convergence[25] and where the possibly more significant anharmonicity of the larger fluctuations in these degrees of freedom may have led to additional error.

Table V shows the ensemble averaged covariance matrix for this internal coordinate set for the $^4C_1$ trajectories. Since the matrix is symmetric, the lower off-diagonal elements are omitted. The diagonal elements of this array represent the mean-square fluctuations for the coordinates in question. As might be expected, the fluctuations in the bond angles are all fairly similar, with the ring C–C–C angles fluctuating less than the C–C–O angles for the hydroxyl oxygen atoms. The fluctuations in θ (10), C4–C5–O5, are somewhat larger than those for the other angles in the ring backbone, again reflecting the greater flexibility in this portion of the molecule. Among the dihedral angles, the largest fluctuations are for the C4–C5–C6–O6 angle, and the smallest are for the C1–C2–C3–C4 and C2–C3–C4–C5 angles, as already noted. It is significant that the matrix is substantially nondiagonal in character, with particularly large covariances for the dihedral angles. It is not surprising that these angles should be highly correlated in a small ring molecule like glucopyranose, but this suggests that approximations which ignore these correlations by computing entropies solely from diagonal elements[26] will not work well here; in fact, considering only the diagonal product gives an entropy difference between the two conformers which is two orders of magnitude too small. The matrix for the $^1C_4$ conformation is similar to the one for $^4C_1$, with many of the diagonal elements being unchanged, within statistical error. The mean-square fluctuations of C4–C5–C6–O6, however, are substantially lower in the $^1C_4$ conformation, and a number of the cross-correlation coefficients for the dihedral angles have changed, as would be expected. As a result, eq 4 gives a value of 1.11 cal/mol·K for the entropy change for the transition from $^1C_4$ to $^4C_1$, or 0.33 kcal/mol at 300 K. Combined with the change in potential energy, and ignoring PV effects, this gives a free-energy change for the transition in vacuum of −2.44 kcal/mol at 300 K. This number

Table V. Mean Covariance Matrix for the Important Coordinates of $^4C_1$ α-D-Glucose as Computed from Molecular Dynamics Simulations

	$\phi(1)$	$\phi(2)$	$\phi(3)$	$\phi(4)$	$\phi(5)$	$\phi(6)$	$\phi(7)$	$\phi(8)$	$\theta(1)$	$\theta(2)$	$\theta(3)$	$\theta(4)$	$\theta(5)$	$\theta(6)$	$\theta(7)$	$\theta(8)$	$\theta(9)$	$\theta(10)$
$\phi(1)$	117.76	88.17	−26.49	−27.87	−15.10	−18.47	30.64	21.02	−3.33	−1.75	−2.47	1.29	−8.96	−2.40	8.46	0.13	0.47	9.53
$\phi(2)$		100.02	−35.73	−42.08	−7.05	−11.25	34.70	21.80	1.94	−7.41	−10.43	0.11	−10.79	−2.40	9.00	0.31	0.57	9.01
$\phi(3)$			80.43	48.94	−14.98	−18.58	−16.97	−11.69	−4.13	4.86	15.13	−6.55	3.88	−0.15	5.99	2.30	0.03	−8.66
$\phi(4)$				62.21	−22.08	−30.98	−10.15	−11.11	−2.79	4.03	15.91	1.62	10.99	1.03	7.34	2.12	−0.05	−9.55
$\phi(5)$					81.96	50.85	−34.32	−16.20	−0.03	−2.17	−6.94	−4.39	−9.87	8.02	−7.84	0.38	−0.98	−11.32
$\phi(6)$						66.16	−44.54	−25.30	−0.07	−0.96	−7.77	−3.07	−10.68	−0.41	−16.14	−1.02	−0.21	−11.30
$\phi(7)$							96.97	41.55	0.70	0.11	−10.80	0.93	8.07	−0.66	17.49	−3.27	−0.50	13.99
$\phi(8)$								309.31	0.11	−0.97	−4.18	0.42	2.58	−5.34	7.08	3.64	0.38	17.87
$\theta(1)$									23.54	−3.74	−1.90	−0.01	0.58	−0.07	−0.67	0.45	0.21	−1.53
$\theta(2)$										22.67	−1.90	1.97	2.85	−0.05	−0.11	−0.28	−0.35	−0.42
$\theta(3)$											18.69	3.25	−6.06	−0.71	1.15	−0.40	0.13	1.27
$\theta(4)$												23.34	−2.28	1.66	1.93	−0.06	−0.08	1.12
$\theta(5)$													17.27	3.22	−6.63	−0.21	0.17	−0.09
$\theta(6)$														22.73	−2.78	1.21	0.72	0.04
$\theta(7)$															18.80	3.61	−0.27	−2.65
$\theta(8)$																21.39	0.71	−3.90
$\theta(9)$																	22.61	0.74
$\theta(10)$																		20.68

(26) Edholm, O.; Berendsen, H. J. C. *Mol. Phys.* **1984**, *51*, 1011.

presumably will be an underestimate, since the calculation has ignored the entropic contributions of the rotating hydroxyl groups, which may be more constrained in the $^1C_4$ conformer, and the greater frequency of conformational transitions of C4–C5–C6–O6 in the $^4C_1$ conformation has not been included. The number also applies only to the molecule in vacuo, not in aqueous solution. Nonetheless, it is in agreement with the experimental observation that the $^4C_1$ conformer is preferred in nature, and with the number estimated for this and similar surfaces using energy minimization studies.[10,13] Angyal[27] calculated a value of −4.15 kcal/mol for this transition in aqueous solution, and Dunfield and Whittington[28] have estimated the vacuum value to be −0.97 kcal/mol. While the entropic contribution is small compared to the enthalpic term (only 13.5% of the total free energy difference), it is not necessarily negligible, as assumed in ref 13.

This method was also used to compute the configurational entropy difference between the gauche (−60°) and anti orientations for the exocyclic dihedral C4–C5–C6–O6 for the $^4C_1$ conformation. Since only about 38 and 55% as much trajectory time, respectively, is available for averaging for these two conformers, the statistical convergence of the resulting number will be correspondingly poorer. It should also be remembered that since the anti conformer is at a lower potential energy, it should be at a higher temperature in a fixed-energy simulation. In these simulations, the anti conformer was approximately 1.8 K hotter than the gauche (−60°) conformer. Using eq 4, the entropy change in going from gauche to anti was estimated to be −0.43 cal/mol·K, or −0.13 kcal/mol at 300 K. This result, if correct in sign, is somewhat surprising, since an intramolecular hydrogen bond might be expected to restrict internal fluctuations. It is clear that the configurational entropy difference between these two states would be affected by the presence of solvent.

IV. Conclusions

These preliminary trajectory studies demonstrate the utility of molecular dynamics simulations in the study of carbohydrate structure, and indicate the need for similar calculations of such molecules in aqueous solution. The most developed of the proposed potential energy surfaces for glucose was tested and found to adequately describe the molecule's motions in vacuo, with small but possibly significant deviations from the crystal geometry. Far from being rigid, these pyranose rings were found to exhibit considerable flexibility, and even to undergo conformational transitions. The relative probabilities of the three major exocyclic group conformers calculated from these trajectories are not in quantitative agreement with the limited experimental data available, but do seem to support previous models of intramolecular hydrogen bonding opposed by unfavorable "syn-axial" interactions. The results of trajectory simulations were also used to estimate the free energy for conformation transition for glucose in vacuo, and to follow the time course of such transitions. These results can be used to evaluate the conformational effects of solvation when solution calculations, currently beginning, are completed.

Acknowledgment. The author thanks Martin Karplus, Louise Berner, and Karen Walker for helpful discussions. This work was supported by Grant No. GM 34970 from the NIGMS.

Registry No. α-D-Glucopyranose, 492-62-6.

(27) Angyal, S. J. *Aust. J. Chem.* **1968**, *21*, 2737.
(28) Dunfield, L. G.; Whittington, S. G. *J. Chem. Soc., Perkin Trans. 2* **1977**, 654.
(29) Brown, G. M.; Levy, H. A., *Acta Crystallogr., Sect. B: Struct. Sci.* **1979**, *35*, 656.

Mechanism of the Photodissociation of *s*-Tetrazine: A Unimolecular Triple Dissociation

Andrew C. Scheiner, Gustavo E. Scuseria, and Henry F. Schaefer III*

Contribution from the Department of Chemistry, University of California, Berkeley, California 94720. *Received May 12, 1986*

Abstract: The triple dissociation of *s*-tetrazine to HCN + HCN + N_2 has been investigated by ab initio molecular electronic structure theory. The predicted activation energy along the ground-state potential energy hypersurface is 47 kcal, consistent with a one-photon excitation to S_1 (51.8 kcal), followed by radiationless transition to vibrationally excited S_0, and finally by unimolecular triple dissociation.

The symmetric tetraaza-substituted benzene, *s*-tetrazine, has been of interest to chemists for nearly 80 years, with the original studies of this red crystalline heterocycle carried out by Curtius, Darapsky, and Müller[1] in 1907 and Koenigsberger and Vogt[2] in 1913. Since that time much effort has been devoted to the characterization of the ground and excited electronic states of *s*-tetrazine. These studies have led in turn to the experimental examination of the dynamics and dissociative photochemistry of electronically excited *s*-tetrazine.

Perhaps most fascinating among the various photochemical findings for *s*-tetrazine is the appearance of very simple dissociation products, namely, molecular nitrogen and hydrogen cyanide. This was first suggested in the 1975 paper by Hochstrasser and King[3] who observed in mixed crystal systems the reaction

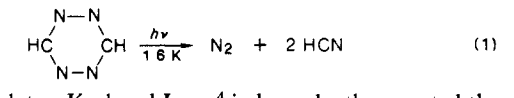

(1)

Three months later, Karl and Innes[4] independently reported the same photochemical reaction in the gas phase. Clearly the mechanism for this decomposition of a medium-sized molecule to three small molecules is of interest, and subsequent studies by Hochstrasser and coworkers pursued this point.[5,6] Other aspects

(1) Curtius, T.; Darapsky, A.; Müller, F. *Chem. Ber.* **1907**, *40*, 84.
(2) Koenigsberger, J.; Vogt, K. *Phys. Z.*, **1913**, *14*, 1269.
(3) Hochstrasser, R. M.; King, D. S. *J. Am. Chem. Soc.* **1975**, *97*, 4760.
(4) Karl, R. R.; Innes, K. K. *Chem. Phys. Lett.* **1975**, *36*, 275.
(5) King, D. S.; Denny, C. T.; Hochstrasser, R. M.; Smith, A. B. *J. Am. Chem. Soc.* **1977**, *99*, 271.
(6) Hochstrasser, R. M.; King, D. S. *J. Am. Chem. Soc.* **1976**, *98*, 5443. (b) Hochstrasser, R. M.; King, D. S.; Smith, A. B. *Ibid.* **1977**, *99*, 3923. (c) Dellinger, B.; King, D. S.; Hochstrasser, R. M.; Smith, A. B. *Ibid.* **1977**, *99*, 3197, 7138. (d) Paczkowski, M.; Pierce, R.; Smith, A. B.; Hochstrasser, R. M. *Chem. Phys. Lett.* **1980**, *72*, 5.

0002-7863/86/1508-8160$01.50/0